Effects of subducted seamounts on megathrust earthquake nucleation and rupture propagation

Hongfeng Yang,[1] Yajing Liu,[1,2] and Jian Lin[1]

Received 14 September 2012; revised 5 November 2012; accepted 5 November 2012; published 19 December 2012.

[1] Subducted seamounts have been linked to interplate earthquakes, but their specific effects on earthquake mechanism remain controversial. A key question is under what conditions a subducted seamount will generate or stop megathrust earthquakes. Here we show results from numerical experiments in the framework of rate- and state-dependent friction law in which a seamount is characterized as a patch of elevated effective normal stress on the thrust interface. We find that whether subducted seamounts generate or impede megathrust earthquakes depends critically on their relative locations to the earthquake nucleation zone defined by depth-variable friction parameters. A seamount may act as a rupture barrier and such barrier effect is most prominent when the seamount sits at an intermediate range of the seamount-to-trench distances (20–100% of the nucleation-zone-to-trench distance). Moreover, we observe that seamount-induced barriers can turn into asperities on which megathrust earthquakes can nucleate at shallow depths and rupture the entire seismogenic zone. These results suggest that a strong barrier patch may not necessarily reduce the maximum size of earthquakes. Instead, the barrier could experience large coseismic slip when it is ruptured. **Citation:** Yang, H., Y. Liu, and J. Lin (2012), Effects of subducted seamounts on megathrust earthquake nucleation and rupture propagation, *Geophys. Res. Lett.*, *39*, L24302, doi:10.1029/2012GL053892.

1. Introduction

[2] Seamounts are ubiquitous topographic features of the seafloor and have profound effects on megathrust earthquakes once they enter subduction zones [*Cloos*, 1992; *Scholz and Small*, 1997; *Watts et al.*, 2010; *Trehu et al.*, 2012]. They have been suggested to lead to additionally frictional resistance on a megathrust interface [*Scholz and Small*, 1997]. Such high-resistance areas may act as asperities where large earthquakes nucleate [*Cloos*, 1992; *Husen et al.*, 2002; *Bilek et al.*, 2003; *Hicks et al.*, 2012], or as barriers that inhibit coseismic rupture propagation [*Kodaira et al.*, 2000]. If such strong barriers are broken, they may induce large coseismic slip concentrated in the barrier region as suggested for the 2011 off Tohoku, Japan Mw 9.0 earthquake [*Simons et al.*, 2011; *Duan*, 2012]. On the other hand, subducted seamounts have also been suggested to be associated with lower interplate coupling due to the presence of entrained fluid-rich sediments on the top of seamounts [*Mochizuki et al.*, 2008; *Singh et al.*, 2011], which may stop ruptures but do not generate large earthquakes. Furthermore, it was proposed that a seamount may generate a complex fracture network in its vicinity, which is unfavorable for the generation of large earthquakes [*Wang and Bilek*, 2011]. Thus the effect of subducted seamounts on megathrust earthquakes could be complex and remains open for debate. In this study we develop a generic subduction fault model to quantitatively evaluate the effect of a seamount on megathrust earthquakes. Assuming that a subducted seamount increases the local normal stress on the fault, we investigate what parameters of a seamount, e.g., its size and relative location, control its effect on megathrust earthquake nucleation and rupture propagation.

2. Method and Model Parameters

[3] We simulate slip and stress evolution during earthquake cycles on a 2D planar thrust fault, similar to previous numerical studies of earthquake sequences in subduction zones [*Stuart*, 1988; *Kato and Hirasawa*, 1997]. The fault is embedded in a homogeneous elastic half space, dips at 12°, and extends 240 km in the down-dip distance. The elastic domains have a shear wave velocity of 3.0 km/s, shear modulus of 30 GPa, and Poisson's ratio of 0.25. A constant long-term plate convergence rate of V_{pl} = 37 mm/yr is imposed at the down-dip end of the fault. Our numerical experiments are performed in the framework of rate- and state-dependent friction [*Dieterich*, 1979; *Ruina*, 1983], with the "ageing" evolution law:

$$\tau = \bar{\sigma} f = (\sigma - p)\left[f_0 + a\ln\left(\frac{V}{V_0}\right) + b\ln\left(\frac{V_o\theta}{d_c}\right)\right], \quad (1)$$

$$\frac{d\theta}{dt} = 1 - \frac{V\theta}{d_c}, \quad (2)$$

where effective normal stress $\bar{\sigma}$ is the difference between normal stress σ and pore pressure p, a and b are rate and state friction stability parameters, V_0 is a reference velocity, d_c is the critical slip distance, f_0 is the nominal friction at steady state when $V = V_0$, and θ is the state variable. Friction stability parameter $a - b$ defines the velocity-weakening (VW, $a - b < 0$, potentially unstable) and velocity-strengthening (VS, $a - b > 0$, stable) regimes on the fault. Stress transmission between fault segments is computed quasi-dynamically using the solutions of stress induced by shear dislocation in an

[1]Department of Geology and Geophysics, Woods Hole Oceanographic Institution, Woods Hole, Massachusetts, USA.
[2]Department of Earth and Planetary Sciences, McGill University, Montreal, Quebec, Canada.

Corresponding author: H. Yang, Department of Geology and Geophysics, Woods Hole Oceanographic Institution, 360 Woods Hole Rd., Woods Hole, MA 02543, USA. (hyang@whoi.edu)

0094-8276/12/2012GL053892

Table 1. Values of $a - b$ and a at Depth[a]

Depth (km)	$a - b$	a
0	0.004	0.0136575
2.9	−0.004	0.0186575
15.7	−0.004	0.0311575
19	0.025	0.0336575
40	0.06	0.0386575

[a]Linear interpolation was applied between pivotal points.

elastic half space [*Okada*, 1992] and a radiation damping term that assures the governing equations continue to have well-defined solutions during slip at seismic rates [*Rice*, 1993]. Although details of rupture propagation such as slip velocity and rupture speed are different for the quasi-dynamic and full-dynamic solutions, qualitative earthquake behaviors such as earthquake nucleation and rupture extent are similar as shown in a direct comparison between these two approaches [*Lapusta and Rice*, 2003]. Thus, the quasi-dynamic approach is appropriate for our investigation on the nucleation and extent of rupture propagation under the influence of seamounts.

[4] The rate and state friction parameter $a - b$ along the subduction fault is converted from temperature-dependent wet granite friction data [*Blanpied et al.*, 1998] using a Cascadia thermal model [*Peacock et al.*, 2002], following *Liu and Rice* [2007]. Table 1 lists their values at depth. Normal stress on the fault is assumed as $\sigma = \rho_c g z$, where ρ_c is density of crust, g is gravitational acceleration, and z is depth. Pore pressure p in subduction zones has been proposed as over-hydrostatic, even near-lithostatic at the up-dip and down-dip ends of the seismogenic zone [*Saffer and Tobin*, 2011]. We here use a constant effective normal stress at depth for simplicity (e.g., $\bar{\sigma} = 50$ MPa) [*Rice*, 1992]. In addition, the effective normal stress is taken to be time-constant, thus does not incorporate any potential pore pressure changes induced by dilatancy or thermal pressurization during fault slip [*Liu and Rubin*, 2010; *Segall et al.*, 2010; *Noda and Lapusta*, 2010].

[5] In our model a seamount is approximated by a strong patch with an elevated effective normal stress $\Delta\bar{\sigma}$ from the background $\bar{\sigma}$ (Figure 1). The amplitude of $\Delta\bar{\sigma}$ is proportional to the height of the seamount, or more precisely, the seamount-induced flexural displacement of the upper plate [*Scholz and Small*, 1997]. Assuming the seamount will flex the upper plate by Δh, $\Delta\bar{\sigma}$ is approximately $C\frac{\Delta h D}{w^4}$, where D is flexural rigidity of the upper plate, w is basal width of the seamount, and C is a constant in the range of 1/3 to 1 associated with pore pressure variation [*Scholz and Small*, 1997]. The range of Δh depends on the sediment thickness in the subduction channel and properties of the overriding plate [*Watts et al.*, 2010]. By assuming a flexural displacement up to half of the seamount height for sediment-starved arcs with little accretionary prism, *Scholz and Small* [1997] estimated $\Delta\bar{\sigma} = 100$ MPa for a 4-km-high and 60-km-wide seamount. If the upper plate is composed of accretionary sediments, $\Delta\bar{\sigma}$ could be smaller [*Honkura et al.*, 1999]. However, shearing off seamounts during subduction will smear out the excess mass and redistribute the elevated normal stress over a broader area, resulting in $\Delta\bar{\sigma}$ of orders of magnitude smaller, e.g., 6.5 MPa [*Scholz and Small*, 1997]. Therefore we examine the sensitivity of our results to the seamount-induced $\Delta\bar{\sigma}$ in the range of 0 to 200 MPa.

[6] Generally seamounts have sizes ranging from a few to tens of kilometers in width. Subducted seamounts have been discovered at depths from a few km to 40 km [*Watts et al.*, 2010; *Singh et al.*, 2011]. Therefore, we model a seamount with different sizes from a very shallow depth to the down-dip VS zone. In order to compare and apply our results to a wide range of subduction zone models and rock rheology, we adopt dimensionless quantities for the down-dip distance d_0 and basal width w of a seamount, $d^* = \frac{d_0}{L}$, $w^* = \frac{w}{L}$, where L is the distance between the trench and the up-dip edge of the earthquake nucleation zone in the reference model (L ≈ 50 km Figure 2a). Consequently, we define the dimensionless down-dip distance on the fault, $x^* = \frac{x}{L}$, where x is the down-dip distance (0–240 km). We also use $\sigma^* = \Delta\bar{\sigma}/\bar{\sigma}$ to represent

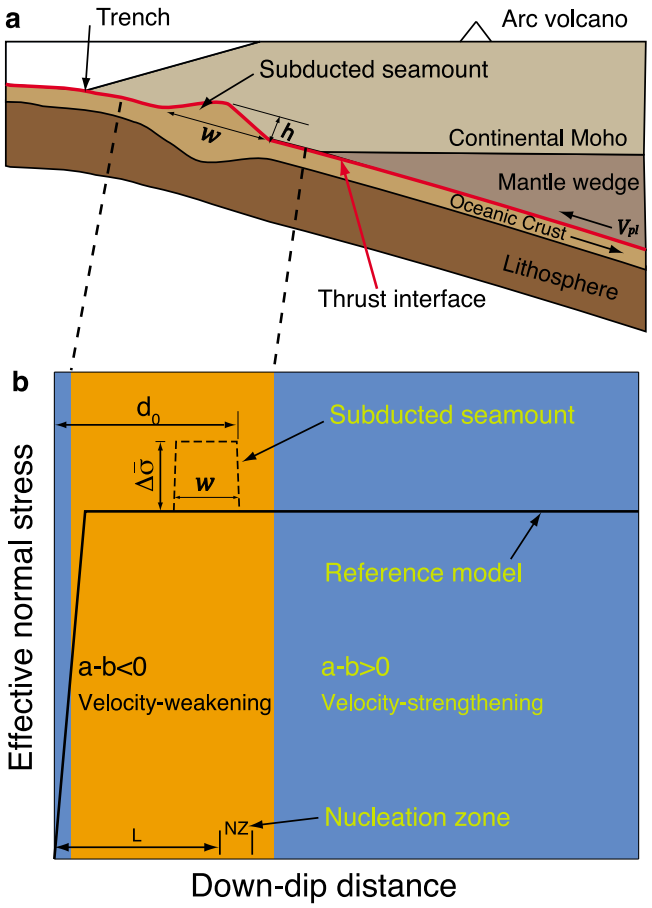

Figure 1. Schematic plot of a subducted seamount. (a) h, seamount peak height. w, seamount basal width. V_{pl}, plate convergence rate. (b) Background effective normal stress $\bar{\sigma}$ (solid line) and perturbation $\Delta\bar{\sigma}$ caused by the subducted seamount (dashed line). d_0 is the distance from trench axis to down-dip edge of the seamount. L is the distance from trench to up-dip edge of the earthquake nucleation zone. Orange color represents velocity-weakening region ($a - b < 0$, capable of generating earthquakes), while blue corresponds to velocity-strengthening segment ($a - b > 0$, stable slip) of the megathrust fault.

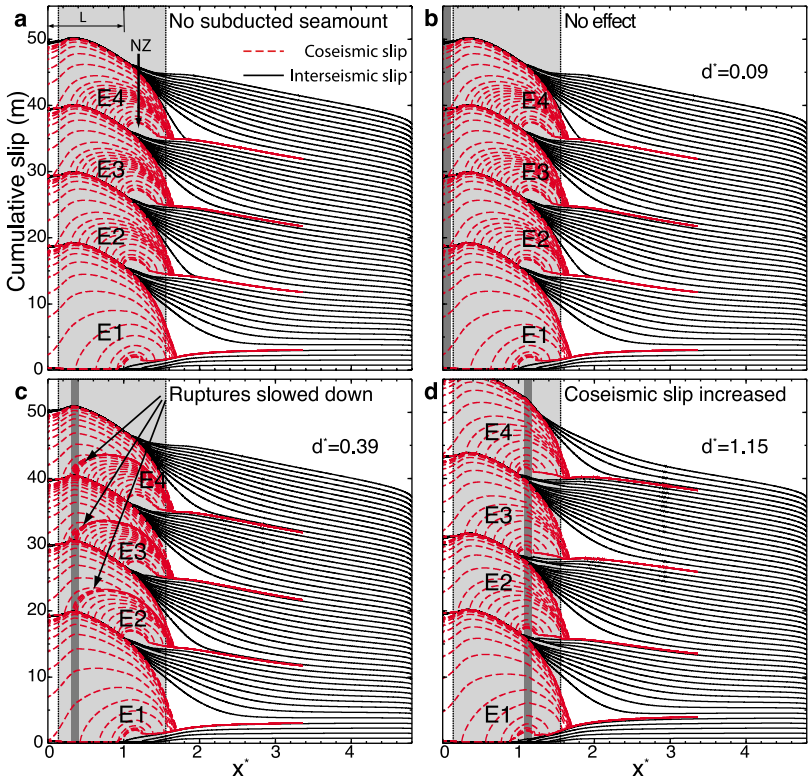

Figure 2. Role of the normalized seamount-trench distance, d^*, on the barrier effect. Cumulative coseismic slip (red dashed lines) for every 10 s and interseismic slip (black lines) for every 20 years on the fault. Light grey area shows velocity-weakening zone. NZ: nucleation zone. L is the distance from trench to the up-dip end of the nucleation zone (L = 50 km). Dark vertical grey bar denotes a subducted seamount of normalized width w^* = 0.06. An effective normal stress increase σ^* = 0.4 is perturbed on background stress level of $\bar{\sigma}$ = 50 MPa. E1–E4 denote earthquake events. (a) No seamount. (b) d^* = 0.09; nearly no effect on ruptures. (c) d^* = 0.39; ruptures of E2, E3, and E4 are slowed down. (d) d^* = 1.15; coseismic slip is increased.

the non-dimensional amplitude of the increase in effective normal stress induced by the seamount.

3. Results

[7] We investigate the role of seamount on earthquakes by changing d^* from 0 to 1.8, w^* from 0 to 1.0, and σ^* in the range of 0 to 4. Simulation results of a reference case without seamount show four megathrust earthquakes for the simulated 1,000 years (Figure 2a). Ruptures nucleate at approximately x^* = 1 and break the entire VW zone. The fault at greater depth slips stably under VS condition.

[8] In the experiments with a seamount, we find that its down-dip location d^* is a critical parameter for the seamount to act as a barrier. *Honkura et al.* [1999] suggested that a seamount at shallow depth might prevent ruptures from breaking to the trench, thus reducing the tsunamigenic potential. In our model with a small up-dip VS zone, however, a shallow seamount sitting up-dip or near the shallow VS-to-VW transition zone ($d^* < 0.2$) cannot stop ruptures (Figure 2b). A seamount can significantly slow down or even stop ruptures if it is subducted to an intermediate distance above the nucleation zone ($0.2 < d^* < 1.0$) (Figures 2c and 4). For a seamount subducted further down-dip into the nucleation zone, ruptures propagate through the VW area without significantly slowing down, resulting in higher coseismic slips (Figure 2d). If a seamount has subducted beyond the VW zone, then it has nearly no effect on earthquake ruptures (Figure S1 in the auxiliary material).[1]

[9] The amplitude of σ^* also plays an important role on the barrier effect (Figure 3). At a given seamount location, a greater value of σ^* makes a seamount more likely to be able to stop ruptures unless d^* is too small. As stated above, a shallow subducted seamount cannot impede ruptures even with an extreme value of $\sigma^* = 4$. In the intermediate range of the seamount-to-trench distance, however, a much smaller σ^* would make the seamount a barrier. The minimum σ^* that is required for a seamount to stop at least one rupture in a sequence of modeled earthquakes also depends on the seamount width (Figure 3b). In our simulation, it is easier for a larger seamount to impede a rupture. Our results show that a seamount is able to stop ruptures in the normalized down-dip distance $d^* \sim 0.5$–1 with $\sigma^* = 0.1$ (Figure 3c). Taking the upper plate properties assumed by *Scholz and Small* [1997], $\Delta\bar{\sigma}$ = 5 MPa ($\sigma^* = 0.1$) translates to tens of meters of flexural displacement of the upper plate for a large seamount, e.g., w = 40 km.

[10] In addition to acting as a barrier, a subducted seamount may also change the location where ruptures nucleate on a megathrust. For instance, we consider a seamount of w^* = 0.24 subducted to d^* = 0.75 (Figure S2). With $\sigma^* = 0.1$,

[1]Auxiliary materials are available in the HTML. doi:10.1029/2012GL053892.

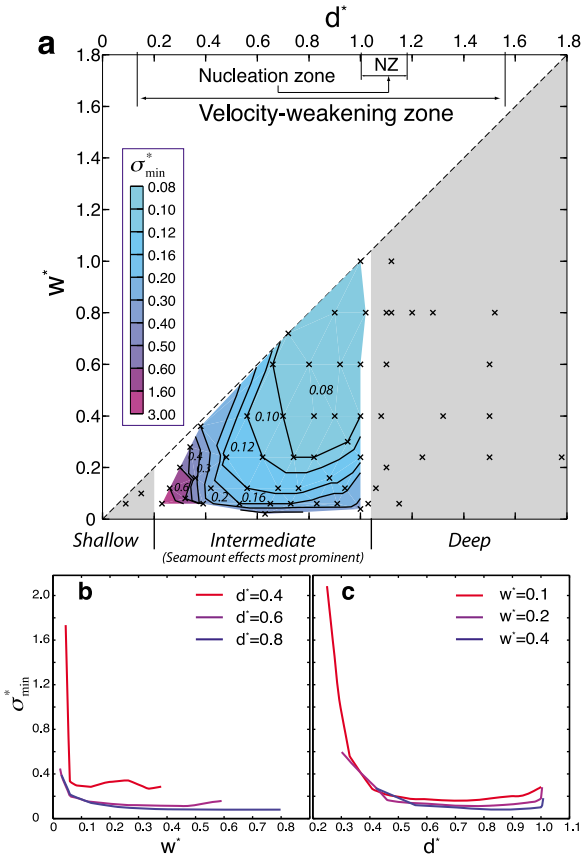

Figure 3. A diagram of w^*, d^*, and σ^*_{min}. (a) Color contour shows the minimum increase in the effective normal stress, σ^*_{min}, required to completely stop at least one megathrust rupture during the simulated 1,000 years. Grey areas denote seamount locations that are unable to stop ruptures for σ^* up to 4. Black crosses represent all the simulation runs. NZ: nucleation zone of megathrust earthquakes without seamounts. (b) Dependence of σ^*_{min} on seamount width w^* for different seamount-trench distance d^*. (c) Dependence of σ^*_{min} on d^* for different seamount widths.

the seamount inhibits ruptures of Events 3 and 5 (Figure S2a). Consequently, post-seismic and inter-seismic shear stresses up-dip of the barrier are increased (Figure S2b), which led to the nucleation of Event 4 in the shallow part of the VW region. This is consistent with the static stress transfer induced seismicity on continental faults [*King et al.*, 1994]. Rupture of Event 4 appears to be slow and does not break the entire VW region because most tectonic stresses there have already been released by previous events (Figure S2b). However, the seamount does not always stop ruptures and could be swept by a large megathrust earthquake, e.g., Event 6 (Figure S2a).

[11] Furthermore, the seamount may become an asperity that initiates megathrust earthquakes (Figure 4). Event 4 is stopped by the seamount, but ~30 minutes later another earthquake (Event 5) initiates on the seamount and ruptures the entire VW zone (Figure 4). Similar features are also found for seamounts of different sizes and locations (Figure S3). This illustrates that megathrust earthquake could initiate on a subducted seamount, as was suggested as a source for the 1990 M_w 7.0 earthquake in the Gulf of Nicoya, Costa Rica [*Husen et al.*, 2002]. If the seamount is located at a shallow depth, as in Figure 4, shallow megathrust earthquake nucleation may also become plausible, contrary to the conventional view that large earthquakes always nucleate near the base of the seismogenic zone [*Das and Scholz*, 1983].

4. Discussion

[12] In our generic model, we have used wet granite friction data, which are most systematically documented in fault-sliding laboratory experiments and most commonly adopted in numerical studies of earthquake nucleation and earthquake cycles. Application of different rock friction properties, such

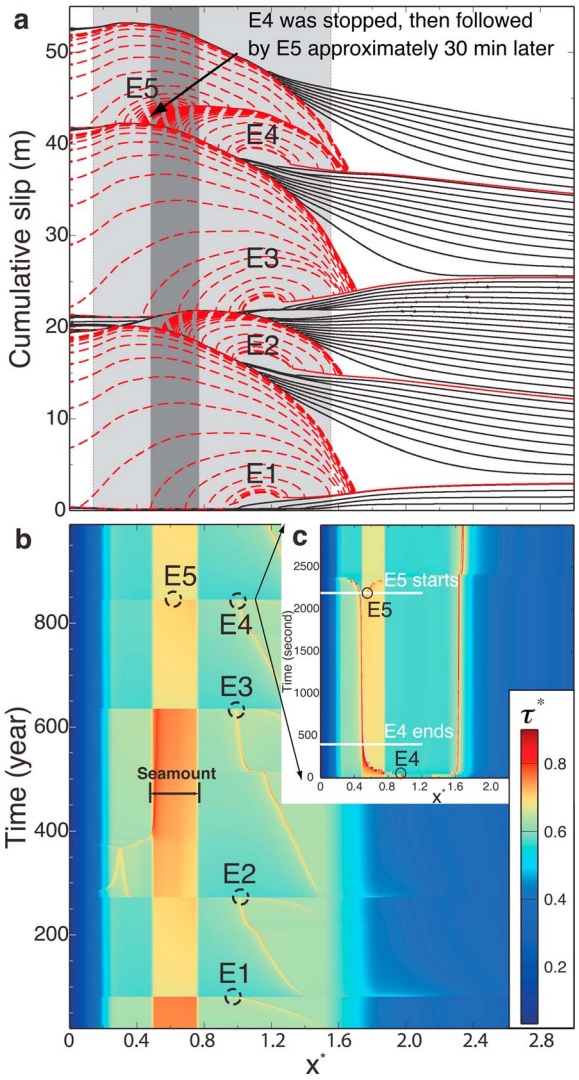

Figure 4. Seamount acting as an asperity. (a) Same as Figure 2 except for a seamount of $w^* = 0.24$, $d^* = 0.75$, and $\sigma^* = 0.2$. Ruptures of E2 and E4 are stopped. E5 is nucleated on the seamount. (b) Color represents interseismic shear stress history. E1–E5 refer to earthquake events. Dashed circles mark the maximum shear stress, $\tau^* = \tau/\bar{\sigma}$, on the fault before each earthquake. (c) A zoom-in view of the shear stress after E4. Circles represent the earthquake nucleation locations. White horizontal lines show ending time of E4 and starting time of E5, respectively.

as gabbro or olivine, in the current model will change the depth distribution of friction parameters and hence the size of the VS and VW zones. For example, application of the hydrothermal gabbro gouge friction data [*He et al.*, 2007] leads to a VW-to-VS transition at a greater depth and a much broader transition zone than that using the wet granite data [*Liu and Rice*, 2009]. The nucleation depth, amplitude of coseismic slip, and recurrence interval of megathrust earthquakes are consequently different. However, the qualitative behaviors such as a coseismic rupture impeded by a highly compressed patch (seamount) are similar (Figure S4), and the main conclusions of this study remain valid.

[13] Subducted seamounts may also weaken the coupling between the overriding and downgoing plates due to the presence of entrained fluid-rich sediments [*Mochizuki et al.*, 2008; *Singh et al.*, 2011]. The sediments in the vicinity of a seamount may increase the local thickness of the gouge layer on the megathrust fault. A thicker fault gouge could stabilize slip and thus impede rupture propagation due to an increase in the friction stability parameter $a - b$ and/or an increase in the characteristic slip distance d_c [*Marone*, 1998]. *Kaneko et al.* [2010] have investigated the relation between interseismic coupling and earthquake rupture patterns through numerical experiments, in which a VS patch separated two VW segments along the strike direction. They found that the VS patch could also be broken by accumulated stress due to ruptures on the neighboring segments. The probability for an earthquake to break through the VS patch was shown to correlate with the average degree of interseismic coupling. Although we have considered a seamount as a strong patch on the fault, our results show that the seamount may not act as a permanent barrier (i.e., one that always stops ruptures) in earthquake cycles.

5. Conclusions

[14] Our model has produced rich earthquake phenomena, including rupture barrier, stress transfer, and nucleation of megathrust earthquakes at relatively shallow depth, despite the simple model approach to treat a subducted seamount as a patch under a higher normal stress. The presented work clearly shows that the distance between a subducted seamount and the earthquake nucleation zone, as defined by depth-dependent rate and state friction parameters, is a key factor to determine whether seamounts would stop or generate megathrust earthquakes. When it is located at shallow depth or deeper than the seismogenic zone on a megathrust, the seamount has little effect on megathrust earthquakes. If it sits in the intermediate distance range up-dip of the nucleation zone, however, the seamount can inhibit or nucleate earthquake ruptures depending on the stress conditions. Our results thus provide insights into understanding the role of mechanical heterogeneities in subduction zone seismic cycles.

[15] **Acknowledgments.** This work is supported by the NSF Grant EAR-1015221 and WHOI Deep Ocean Exploration Institute awards 27071150 and 25051162. We benefited from discussion with Pablo Canales, Yoshihiro Kaneko, Min Xu, and the WHOI Marine Tectonics Group. We are grateful to Anne Trehu and one anonymous reviewer for providing insightful comments, which have improved the paper.

[16] The Editor thanks Ann Trehu and an anonymous reviewer for their assistance in evaluating this paper.

References

Bilek, S. L., S. Y. Schwartz, and H. DeShon (2003), Control of seafloor roughness on earthquake rupture behavior, *Geol. Soc. Am. Bull.*, *31*, 455–458.

Blanpied, M. L., C. J. Marone, D. A. Lockner, J. D. Byerlee, and D. P. King (1998), Quantitative measure of the variation in fault rheology due to fluid-rock interactions, *J. Geophys. Res.*, *103*, 9691–9712, doi:10.1029/98JB00162.

Cloos, M. (1992), Thrust-type subduction-zone earthquakes and seamount asperities: A physical model for seismic rupture, *Geology*, *20*, 601–604, doi:10.1130/0091-7613(1992)020<0601:TTSZEA>2.3.CO;2.

Das, S., and C. H. Scholz (1983), Why large earthquakes do not nucleate at shallow depths, *Nature*, *305*, 621–623, doi:10.1038/305621a0.

Dieterich, J. H. (1979), Modeling of rock friction: 1. Experimental results and constitutive equations, *J. Geophys. Res.*, *84*, 2161–2168, doi:10.1029/JB084iB05p02161.

Duan, B. (2012), Dynamic rupture of the 2011 Mw 9.0 Tohoku-Oki earthquake: Roles of a possible subducting seamount, *J. Geophys. Res.*, *117*, B05311, doi:10.1029/2011JB009124.

He, C., Z. Wang, and W. Yao (2007), Frictional sliding of gabbro gouge under hydrothermal conditions, *Tectonophysics*, *445*, 353–362, doi:10.1016/j.tecto.2007.09.008.

Hicks, S. P., A. Rietbrock, C. A. Haberland, I. M. A. Ryder, M. Simons, and A. Tassara (2012), The 2010 Mw 8.8 Maule, Chile earthquake: Nucleation and rupture propagation controlled by a subducted topographic high, *Geophys. Res. Lett.*, *39*, L19308, doi:10.1029/2012GL053184.

Honkura, Y., Y. Nagaya, and H. Kuroki (1999), Effects of seamounts on an interplate earthquake at the Suruga Trough, Japan, *Earth Planets Space*, *51*, 449–454.

Husen, S., E. Kissling, and R. Quintero (2002), Tomographic evidence for a subducted seamount beneath the Gulf of Nicoya, Costa Rica: The cause of the 1990 Mw = 7.0 Gulf of Nicoya earthquake, *Geophys. Res. Lett.*, *29*(8), 1238, doi:10.1029/2001GL014045.

Kaneko, Y., J. Avouac, and N. Lapusta (2010), Towards inferring earthquake patterns from geodetic observations of interseismic coupling, *Nat. Geosci.*, *3*, 363–369, doi:10.1038/ngeo843.

Kato, N., and T. Hirasawa (1997), A numerical study on seismic coupling along subduction zones using a laboratory-derived friction law, *Phys. Earth Planet. Inter.*, *102*, 51–68, doi:10.1016/S0031-9201(96)03264-5.

King, G. C. P., R. S. Stein, and J. Lin (1994), Static stress changes and the triggering of earthquakes, *Bull. Seismol. Soc. Am.*, *84*, 935–953.

Kodaira, S., N. Takahashi, A. Nakanishi, S. Miura, and Y. Kaneda (2000), Subducted seamount imaged in the rupture zone of the 1946 Nankaido earthquake, *Science*, *289*, 104–106, doi:10.1126/science.289.5476.104.

Lapusta, N., and J. R. Rice (2003), Nucleation and early seismic propagation of small and large events in a crustal earthquake model, *J. Geophys. Res.*, *108*(B4), 2205, doi:10.1029/2001JB000793.

Liu, Y., and J. R. Rice (2007), Spontaneous and triggered aseismic deformation transients in a subduction fault model, *J. Geophys. Res.*, *112*, B09404, doi:10.1029/2007JB004930.

Liu, Y., and J. R. Rice (2009), Slow slip predictions based on granite and gabbro friction data compared to GPS measurements in northern Cascadia, *J. Geophys. Res.*, *114*, B09407, doi:10.1029/2008JB006142.

Liu, Y., and A. M. Rubin (2010), Role of fault gouge dilatancy on aseismic deformation transients, *J. Geophys. Res.*, *115*, B10414, doi:10.1029/2010JB007522.

Marone, C. (1998), Laboratory-derived friction laws and their application to seismic faulting, *Annu. Rev. Earth Planet. Sci.*, *26*, 643–696, doi:10.1146/annurev.earth.26.1.643.

Mochizuki, K., T. Yamada, M. Shinohara, Y. Yamanaka, and T. Kanazawa (2008), Weak interplate coupling by seamounts and repeating M ~ 7 earthquakes, *Science*, *321*, 1194–1197, doi:10.1126/science.1160250.

Noda, H., and N. Lapusta (2010), Three-dimensional earthquake sequence simulations with evolving temperature and pore pressure due to shear heating: Effect of heterogeneous hydraulic diffusivity, *J. Geophys. Res.*, *115*, B12314, doi:10.1029/2010JB007780.

Okada, Y. (1992), Internal deformation due to shear and tensile faults in a half-space, *Bull. Seismol. Soc. Am.*, *82*, 1018–1040.

Peacock, S. M., K. Wang, and A. M. McMahon (2002), Thermal structure and metamorphism of subducting oceanic crust: Insight into Cascadia intraslab earthquakes, in *The Cascadia Subduction Zone and Related Subduction Systems: Seismic Structure, Intraslab Earthquakes and Processes, and Earthquake Hazards*, edited by S. Kirby, K. Wang, and S. Dunlop, *U.S. Geol. Surv. Open File Rep.*, *02-328*, 123–126.

Rice, J. R. (1992), Fault stress states, pore pressure distributions, and the weakness of the San Andreas Fault, in *Fault Mechanics and Transport Properties in Rocks*, pp. 475–503, Elsevier, New York, doi:10.1016/S0074-6142(08)62835-1.

Rice, J. R. (1993), Spatiotemporal complexity of slip on a fault, *J. Geophys. Res.*, *98*, 9885–9907, doi:10.1029/93JB00191.

Ruina, A. L. (1983), Slip instability and state variable friction laws, *J. Geophys. Res.*, *88*, 10,359–10,370, doi:10.1029/JB088iB12p10359.

Saffer, D. M., and H. J. Tobin (2011), Hydrogeology and mechanics of subduction zone forearcs: Fluid flow and pore pressure, *Annu. Rev. Earth Planet. Sci.*, *39*, 157–186, doi:10.1146/annurev-earth-040610-133408.

Scholz, C. H., and C. Small (1997), The effect of seamount subduction on seismic coupling, *Geology*, *25*, 487–490, doi:10.1130/0091-7613(1997)025<0487:TEOSSO>2.3.CO;2.

Segall, P., A. M. Rubin, A. M. Bradley, and J. R. Rice (2010), Dilatant strengthening as a mechanism for slow slip events, *J. Geophys. Res.*, *115*, B12305, doi:10.1029/2010JB007449.

Simons, M., et al. (2011), The 2011 magnitude 9.0 Tohoku-Oki earthquake: Mosaicking the megathrust from seconds to centuries, *Science*, *332*, 1421–1425, doi:10.1126/science.1206731.

Singh, S. C., et al. (2011), Aseismic zone and earthquake segmentation associated with a deep subducted seamount in Sumatra, *Nat. Geosci.*, *4*, 308–311, doi:10.1038/ngeo1119.

Stuart, W. D. (1988), Forecast model for great earthquakes at the Nankai Trough subduction zone, *Pure Appl. Geophys.*, *126*, 619–641, doi:10.1007/BF00879012.

Trehu, A. M., R. J. Blakely, and M. C. Williams (2012), Subducted seamounts and recent earthquakes beneath the central Cascadia forearc, *Geology*, *40*, 103–106, doi:10.1130/G32460.1.

Wang, K., and S. L. Bilek (2011), Do subducting seamounts generate or stop large earthquakes?, *Geology*, *39*, 819–822, doi:10.1130/G31856.1.

Watts, A. B., A. A. P. Koppers, and D. P. Robinson (2010), Seamount subduction and earthquakes, *Oceanography*, *23*, 166–173, doi:10.5670/oceanog.2010.68.